

Quantitative evaluation of carbonation in concrete using nonlinear ultrasound

Gun Kim · Jin-Yeon Kim · Kimberly E. Kurtis ·
Laurence J. Jacobs · Yann Le Pape ·
Maria Guimaraes

Received: 25 September 2014 / Accepted: 18 December 2014 / Published online: 27 December 2014
© RILEM 2014

Abstract A new nonlinear ultrasonic technique for nondestructive evaluation of concrete components is developed and implemented to characterize the effects of carbonation on concrete. The physical principle of this method is the second harmonic generation (SHG) in propagating Rayleigh surface waves which are detected by a non-contact air-coupled transducer. The nonlinearity parameter, as an indicator of material properties, is experimentally obtained from measured Rayleigh wave signals and is used to quantitatively evaluate the progress of carbonation under accelerated conditions. The experimental results show that there is

a significant decrease in the measured nonlinearity parameter, most likely originated from the deposit of the carbonation product, CaCO_3 , in pre-existing voids and microcracks. The sensitivity of the nonlinearity parameter is also verified by comparing with the measured Rayleigh wave velocity. The results in this paper demonstrate that the SHG technique using Rayleigh surface waves can be used to monitor carbonation in concrete.

Keywords NDE for cement-based materials · Nonlinear Rayleigh waves · Nonlinearity parameter · Carbonation

G. Kim · J.-Y. Kim · K. E. Kurtis · L. J. Jacobs (✉)
School of Civil and Environmental Engineering, Georgia
Institute of Technology, Atlanta, GA 30332-0355, USA
e-mail: laurence.jacobs@ce.gatech.edu

L. J. Jacobs
G. W. Woodruff School of Mechanical Engineering,
Georgia Institute of Technology, Atlanta,
GA 30332-0355, USA

Y. Le Pape
EDF Inc., Chevy Chase, MD, USA

Present Address:
Y. Le Pape
Oak Ridge National Laboratory, Oak Ridge,
TN 37831-6148, USA

M. Guimaraes
Electric Power Research Institute (EPRI), Charlotte,
NC 28262-8550, USA

1 Introduction

Exposure of in-service concrete infrastructure to the natural environment causes continuous changes in microstructure and composition, often starting from their surfaces. It is well known that carbonation is a common occurrence in cement-based materials. During carbonation, calcium hydroxide ($\text{Ca}(\text{OH})_2$) contained in hydrated cement paste reacts with carbon dioxide, present in air or water, forming calcium carbonate (CaCO_3) and water (H_2O). The gradual process of carbonation alters the surface properties and decreases the pH value of the pore solution from typical values (12–13.0) to a 9 or less [1–3] due to the virtually insolubility of the carbonation product

(CaCO₃) relative to the slightly soluble reactant [4]. More recently, processes to intentionally carbonate ordinary Portland cement concrete and concrete produced with alternative cements are of growing interest as potential options for carbon sequestration [5, 6].

However, over time in reinforced concrete, as the relatively low-pH “carbonation front” reaches greater depths from the surface, depassivation of the reinforcement steel can occur and corrosion can initiate. Corrosion of reinforcement is considered to be a serious durability concern which ultimately limits the service life of reinforced concrete structures [7–9].

Hence, for a number of reasons, it is critical to detect carbonation in concrete. Methods to do so non-destructively are preferred such that elements or structures can be monitored over time as carbonation progresses. Also, on large-scale structures, destructive testing is either not permitted or cost-prohibitive and is not capable of providing a representative statistical sampling of the structural condition. Automated monitoring using embarked nondestructive devices is the most promising approach to a full-extent degradation mapping of structures like atmospheric cooling towers or nuclear containment buildings.

Various evaluation methods have been used to detect carbonation in concrete. The use of an indicator solution, like phenolphthalein, is the most well-known method to measure the depth of the carbonation, and this must be done on a freshly fractured surface [3, 10]. Also, analytical methods like thermogravimetric analysis (TGA) [1–3, 11–13] and quantitative X-ray diffraction (QXRD) analysis [11, 14] can be used to assess the relative amount of Ca(OH)₂ and CaCO₃ at various depths in a sample obtained from a structure. Most recently, indentation methods, (i.e., micro [10] and nanoindentation [15]) have been used to characterize carbonation depths and the process of carbonation. Accordingly, it is well-established that carbonation significantly influences density, strength, elasticity moduli, pore size, and permeability among other properties of cement-based materials [16–18]. Research has also been directed toward increasing the durability against carbonation, which has been shown to be controlled by the use of SCMs [10, 19–23], water-to-cement ratio (w/c) [23–26], curing conditions and time [21, 27, 28], aggregate type [8], the different alkali contents [24, 26, 29], and environmental factors [23, 25]. However, in spite of this

extensive research, little effort has been made to use nondestructive evaluation (NDE) methods to evaluate the carbonation process.

NDE techniques using ultrasound have been developed to characterize concrete microstructures [30–33]. Recent research [34–37] introduced nonlinear ultrasonic techniques that can characterize microstructural changes in cement-based materials, such as the formation of microcracks, with more sensitivity than conventional linear ultrasonic methods such as phase velocity or attenuation. For instance, Chen et al. [34] and Leśnicki et al. [35, 36] established the nonlinear impact resonance acoustic spectroscopy (NIRAS) technique based on the shift of the resonance frequency that is caused by material damage; the NIRAS method excites the fundamental resonance of the sample by impact hammer and detects the vibration signal using an accelerometer. They showed that NIRAS can quantify the nonlinear hysteresis of mortar bars with different aggregates, and assessed the influence of progressive alkali-silica reaction (ASR) damage on microstructure using the changes in the measured nonlinearity parameter. Bouchaala et al. [37] also observed a shift of resonance frequencies induced by the carbonation and demonstrated that the measured material nonlinearity appears to be decreased by the progress of carbonation. Nevertheless, these resonance-based techniques are limited to relatively small-sized specimens, so they are impractical for the interrogation of large or complicated components. Also, those resonance methods measure the changes in global damage state of the specimen; the measured nonlinearity in this case represents an averaged value for the entire specimen. On the other hand, the carbonation reaction largely progresses as a relatively uniform front due to the CO₂ penetration from the concrete surface; therefore its product or the changed microstructure is concentrated near the surface. The surface wave-based techniques are well-suited to evaluate material properties such as the density, Poisson’s ratio, and the shear modulus at the surface, where carbonation affects these properties, since the wave’s energy is concentrated near surface. Additionally, the fact that they only need access to one-side of the specimen shows their capability for the application to in situ interrogation of in-service structures.

It has been demonstrated that second harmonic generation (SHG) methods using nonlinear Rayleigh



surface waves [38–44] have great potential. The experimentally obtained acoustic nonlinearity parameter, β , (defined in Eq. (3)) can be related to the microstructural changes caused by damage if a proper model is developed. Furthermore, the unwanted system nonlinearity from the instrumentation can be eliminated by varying the propagation distance. Most recently, Thiele et al. [42] developed an SHG technique by using an air-coupled receiver that allows for a more consistent measurement of the nonlinearity parameter. Kim et al. [38] proposed a similar SHG setup for cement-based materials and assessed the effect of shrinkage-reducing admixture (SRA) on reducing autogenous and drying shrinkage, showing that the measured acoustic nonlinearity parameter is decreased by the addition of SRA.

The objective of this paper is to quantitatively assess the carbonation effect on the microstructure in a prepared concrete specimen using the proposed SHG setup in [38]. Specifically, it is expected that micro-cracks in the specimen—which are inherent defects in cement-based composites [45]—are changed by the evolution of the carbonation which will in turn affect the nonlinearity parameter. A 45 kHz wedge transducer and a 100 kHz air-coupled (non-contact) transducer are implemented to generate and to receive the Rayleigh surface waves, respectively. In order to track the degree of carbonation, a phenolphthalein indicator solution is employed to measure carbonation depths on additional small concrete blocks as a function of days. Finally, the potential and advantages of applying the SHG technique for evaluating carbonation in cement-based materials are discussed.

2 Nonlinearity parameter: second harmonic generation (SHG)

Consider a plane Rayleigh surface wave propagating along the x axis in an isotropic, macroscopically homogeneous, and nonlinear elastic half space where the z axis refers to the depth of the material. First, the displacements in the x and z directions can be written in Eq. (1) and both displacement components indicate the shear and longitudinal wave contributions [46].

$$u_x(\omega) = A_1 \left(e^{b_1 z} - \frac{2b_1 b_2}{k_R^2 + b_2^2} e^{b_2 z} \right) e^{i\{k_R(x - c_R t)\}} \quad (1a)$$

$$u_z(\omega) = iA_1 \frac{b_1}{k_R} \left(e^{b_1 z} - \frac{2k_R^2}{k_R^2 + b_2^2} e^{b_2 z} \right) e^{i\{k_R(x - c_R t)\}}, \quad (1b)$$

where, C_R is the speed of Rayleigh surface waves, ω is the fundamental angular frequency ($=C_R k_R$), $b_1 = \sqrt{k_R^2 - k_1^2}$ and $b_2 = \sqrt{k_R^2 - k_s^2}$ with k_1 , k_s , and k_R are the wave numbers of the longitudinal wave, the shear wave, and the Rayleigh waves.

In an isotropic material that has weak quadratic nonlinearity, the displacements of the second harmonic Rayleigh waves in the far-field can be expressed as [39, 47]:

$$u_x(2\omega) \approx A_2 \left(e^{2b_1 z} - \frac{2b_1 b_2}{k_R^2 + b_2^2} e^{2b_2 z} \right) e^{i\{2k_R(x - c_R t)\}} \quad (2a)$$

$$u_z(2\omega) \approx iA_2 \frac{b_1}{k_R} \left(e^{2b_1 z} - \frac{2k_R^2}{k_R^2 + b_2^2} e^{2b_2 z} \right) e^{i\{2k_R(x - c_R t)\}} \quad (2b)$$

Hermann et al. [39] showed that the acoustic nonlinearity parameter can be expressed by the out-of-plane displacement components of the propagating Rayleigh waves at the surface ($z = 0$) as shown in Eq. (3)

$$\beta = \frac{u_z(2\omega)|_{z=0}}{u_z^2(\omega)|_{z=0}} \frac{8b_1 i}{k_1^2 k_R x} \left(1 - \frac{2k_R^2}{k_R^2 + b_2^2} \right), \quad (3)$$

where, β is the acoustic nonlinearity parameter [39, 47–49]. The relationship between the fundamental and second harmonic components and the acoustic nonlinearity parameter can be written as [47]

$$\frac{A_2}{A_1^2} \propto \frac{\beta \omega^2 x}{C_R^2} \quad (4)$$

Since the wave speed of the Rayleigh surface wave is independent of the frequency of the wave, A_2/A_1^2 is directly proportional to β at a fixed distance as shown in Eq. (5). It is well established that the relationship between A_2/A_1^2 and the propagation distance is a good approximation for calculating the acoustic nonlinearity parameter for short propagation distances

$$\beta \propto \frac{A_2}{A_1^2 x}. \quad (5)$$

This paper denotes $A_2/A_1^2 x$ as the relative nonlinearity parameter, β_{re} as shown in Eq. (6)



$$\beta_{re} = \frac{A_2}{A_1^2 x}. \quad (6)$$

The amplitude of the fundamental (A_1) and second harmonic (A_2) can be experimentally measured using the setup described in the next section. Therefore, the changes in the elastic nonlinearity of a material can be assessed using a nondestructive, macroscopic measurement.

3 Experimental procedure

3.1 Specimen preparation

Based on ACI 211.1 [50], one concrete specimen ($21.5 \times 56.5 \times 17.5$ cm) with Type I Portland cement (ASTM C 150) [51] is prepared for both accelerated carbonation tests and nonlinear ultrasonic (NLU) measurements. River gravel coarse aggregate with a maximum size of aggregate (MSA) of 12.7 mm, and dry rodded unit weight (DRUW) of $1,646 \text{ kg/m}^3$ (103 pcf) and a natural sand with a fineness modulus (FM) of 3.04, absorption capacity of 1.93 %, and saturated surface dry (SSD) specific gravity of 2.65 are used as aggregate. A water-to-cement ratio (w/c) of 0.60 is selected to accelerate the rate and depth of carbonation [24]. Table 1 shows further details on the mixture design of concrete specimen.

The freshly mixed concrete is cast, and cured for 14 days at ambient temperature while covered by polyethylene sheeting. The demolded specimen is then placed in an environmental chamber (23 °C and 95 % relative humidity) in relatively moist conditions to facilitate hydration until it reaches 28 days of age. Finally, the specimen is transferred into an environmental chamber (23 °C and 50 ± 2 % relative humidity) to dry for 14 days to bring it to an equilibrium

moisture condition. Additionally, five concrete blocks, each sealed on 5 sides for one-dimensional penetration of CO_2 , are prepared according to the same mix design and cured and conditioned in the same manner. An indicator solution, 1 % solution of phenolphthalein in deionized water with 10 % v/v ethanol, are prepared for tracking the carbonation depth on freshly cut concrete surfaces.

3.2 Accelerated carbonation experiments

The accelerated carbonation test on the prepared concrete specimen and blocks is carried out for 40 days in a carbonation chamber, with temperature, relative humidity, and CO_2 concentration control. Note that the maximum carbonation rate occurs at approximately 55–65 % RH [2, 52]. In this experiment, the RH is fixed to 55 %. The temperature in the environmental chamber is maintained at 26 °C. During the accelerated carbonation test, a continuous supply of CO_2 gas is maintained by the pressure regulator mounted on the pressurized steel cylinder and 20 % CO_2 is continuously fed into the chamber [10]. In this condition, the increase in carbonation depth due to increases in temperature is negligible [2]; the rate of carbonation is governed by the diffusion of CO_2 . The test is interrupted after 0, 7, 14, 25, and 31 days of exposure so as to estimate the level of carbonation penetration in each block and the phenolphthalein indicator solution is applied to a freshly cut surface.

3.3 Non-contact, nonlinear ultrasonic measurements

The non-contact (air-coupled) measurements of SHG in Rayleigh surface waves are performed with the setup shown in Fig. 1. Details on the experimental procedure to calculate the nonlinearity parameter in concrete are described in [38]. A narrow band longitudinal wave piezoelectric transducer with a diameter of 50 mm (Ultran GRD 50) is employed as a transmitter and is coupled to a Teflon wedge with vacuum grease. The longitudinal wave speed in Teflon is 1,450 m/s and the Rayleigh surface wave speed in the concrete specimen is 2,450 m/s. Therefore the wedge angle for generating the Rayleigh waves in the concrete specimen is 36.3° based on Snell's law. To maximize the detected wave amplitude and to have a

Table 1 Mixture design of concrete specimen, kg/m^3 (lb/yd^3)

	Concrete
Water	271 (365)
Cement (ASTM C150 type I)	361 (608)
Water-to-cement ratio (w/c)	0.60
Coarse aggregate	872 (1,470)
Fine aggregate	784 (1,322)



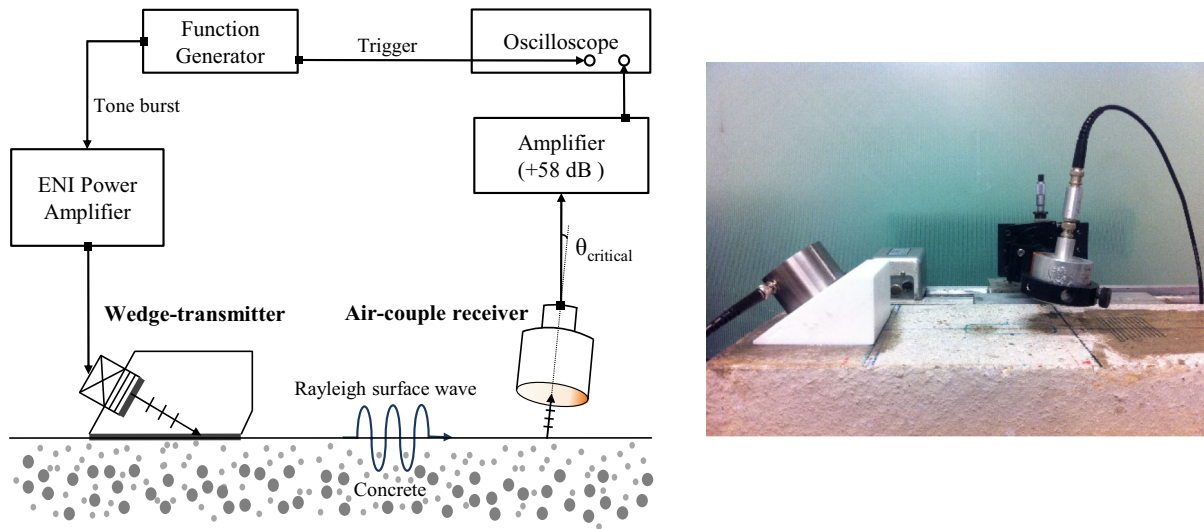


Fig. 1 Air-coupled detection setup for Rayleigh surface waves

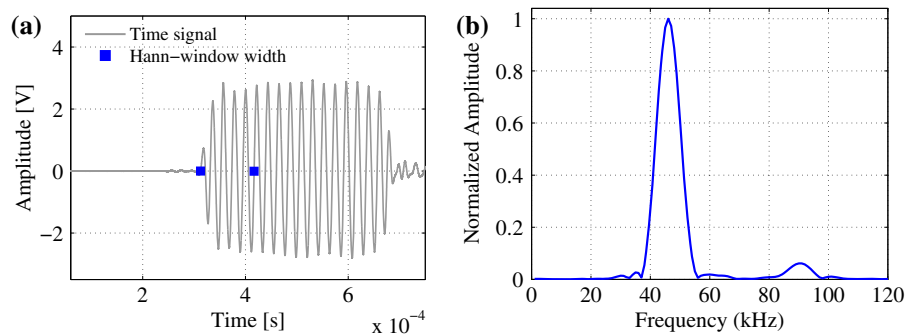


Fig. 2 Time signal and Fourier spectrum for NLU measurement (45 and 90 kHz)

minimum attenuation, the transmitter/wedge assembly is designed in such a way that the wedge's bottom surface is smooth enough and the assembly is tightly coupled to the concrete specimen using the same vacuum grease.

A tone-burst signal of 16 cycles at 45 kHz is generated by a function generator (AGILENT 33250A) with a peak-to-peak voltage of 400 mV and is repeated every 200 ms. Then a power amplifier (ENI Power Amplifier) amplifies the signal as much as 50 dB and the amplified signal is fed to the wedge transmitter. To detect the propagating Rayleigh waves, a non-contact, air-coupled transducer with a diameter of 50 mm (Ultran GRD 100) is used. Here, the air-coupled receiver is tilted by 8° which is the critical angle for the Rayleigh wave at the air-concrete

interface and it is slightly adjusted for small variations of wave speed during the carbonation. Then, the distance between the air-coupled receiver and the surface, called the lift-off distance, is fixed at 3.3 cm. At this distance, one can reduce the effects of attenuation and diffraction in the air [38, 42] while avoiding the multiple reflections of the acoustic signal between the concrete surface and transducer surface. To increase the signal-to-noise ratio (SNR), the received signal is amplified by 58 dB with a broadband preamplifier (Digital Wave Inc.). Additionally, the received time-domain signals are averaged 256 times with an oscilloscope (Tektronix TDS 5034B Digital); the calculated SNR is approximately 50 dB. Finally, the averaged signal is transferred to a computer for post-processing. The entire

measurement is synchronized by a trigger signal from the function generator as shown in Fig. 1. The measurements are repeated 15–20 times.

During the accelerated carbonation process, the specimen is periodically removed from the chamber for the ultrasonic measurements, which are made after 0, 3, 7, 10, 14, 19, 25, 31, and 40 days of carbonation. Since the dimensions of the specimen limits the propagation distance, the propagation distance varies only from 250 to 295 mm by an incremental step of 5 mm. In the post-processing, a Hann window is applied to the first 5 cycles of the received time domain signals since it is expected that the boundary-reflected waves arrive at approximately 42 ms (the 6th cycle) and this reflected signal interferes with the directly propagating Rayleigh wave. It should be noted that it has been experimentally demonstrated that the first 5 cycles are not affected by these reflected waves [38]. Figure 2a shows the width of the Hann window (denoted by the blue squares) as well as the received time domain signal, and Fig. 2b shows the measured amplitudes of the fundamental (A_1) and second harmonic (A_2) from the frequency spectrum of the windowed signal obtained using the fast Fourier transform (FFT).

Figures 3 and 4 show an example of the measured A_1 , A_2 , and A_2/A_1^2 versus propagation distance on the concrete specimen cured for 31 days in the carbonation chamber. Obviously, the measured fundamental amplitude, A_1 tends to decrease with propagation distance mainly due to the beam spreading and attenuation effects in concrete. On the other hand, due to the cumulative nonlinear effects described in [53], the second harmonic amplitude, A_2 increases with propagation distance. Figure 4 shows that A_2/A_1^2

increases linearly with propagation distance, and the increase in A_2/A_1^2 is in agreement with previous experimental observations [38–44].

4 Results and discussion

4.1 Carbonation profile using phenolphthalein indicator solution

First, the destructive tests are performed to determine the carbonation depth. The indicator is sprayed uniformly on each freshly broken surface of the carbonated blocks after 0, 7, 14, 25, and 31 days of carbonation in the chamber. The results show that the uncarbonated area, of pH higher than approximately 9.2, appears as purple, while the carbonated area remains colorless. Figure 5 shows the photographs of each cross-section of the carbonated blocks. The depth of carbonation is then measured by averaging at 7 points perpendicular to one face of the split concrete blocks, and the measured depths are 1.7, 9, 14, 18, and

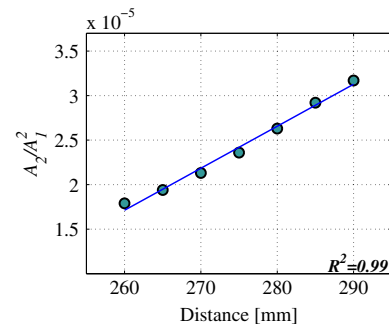


Fig. 4 A_2/A_1^2 versus propagation distance

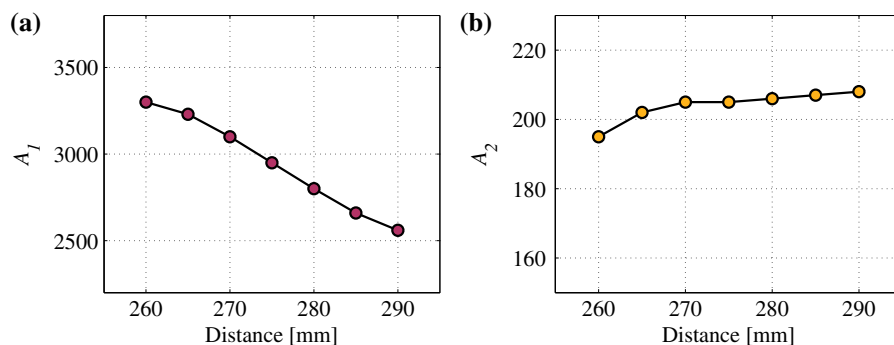


Fig. 3 The measured fundamental and second harmonic amplitudes of nonlinear Rayleigh surface waves



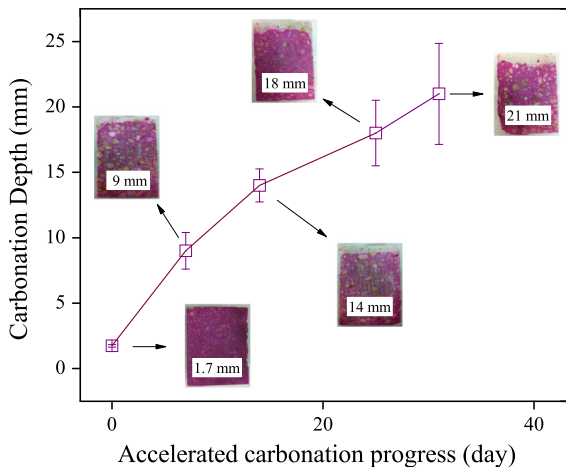


Fig. 5 Averaged carbonation depth using phenolphthalein indicator solution

21 mm, respectively. As a result, it is determined that the carbonation depth is nonlinearly increased over time, as expected [10].

4.2 Linear ultrasonic parameter (phase velocity) results

The phase velocity is measured using the time domain signals received at two different propagation distances. The distance between the two measurement positions is divided by the difference in arrival times to obtain the phase velocity. The resulting phase velocities during the carbonation process are shown in Fig. 6 and Table 2. It is interesting to note that the measured phase velocity increases with the carbonation process. This increase suggests that the elastic moduli in fact increase more than the increase in density by the CaCO_3 formation. However, the results show only a maximum of 5.5 % change during the curing for 40 days. Furthermore, the changes in phase velocity are comparable to the measurement error bars. For these reasons, it is difficult to use the phase velocity as an indicator to detect microstructural changes due to the carbonation reaction.

Additionally, it is confirmed that the concrete specimen can be treated as a weakly dispersive medium, in agreement with the results of [38], since the phase velocity for the specimen at each carbonation state is almost constant within the effective frequency range (approximately 40–100 kHz). This is important since the carbonation layer could cause

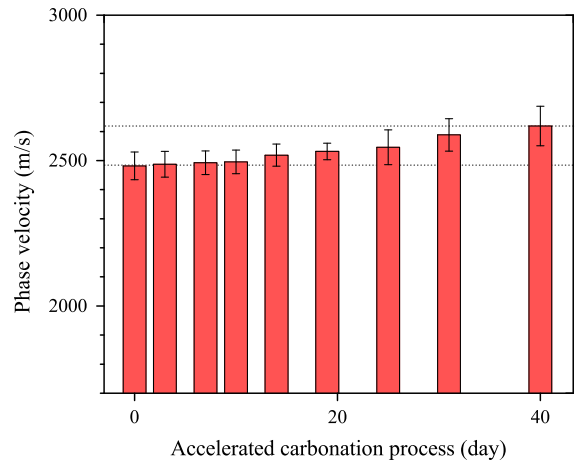


Fig. 6 Trend of measured Rayleigh phase velocity with the accelerated carbonation tests

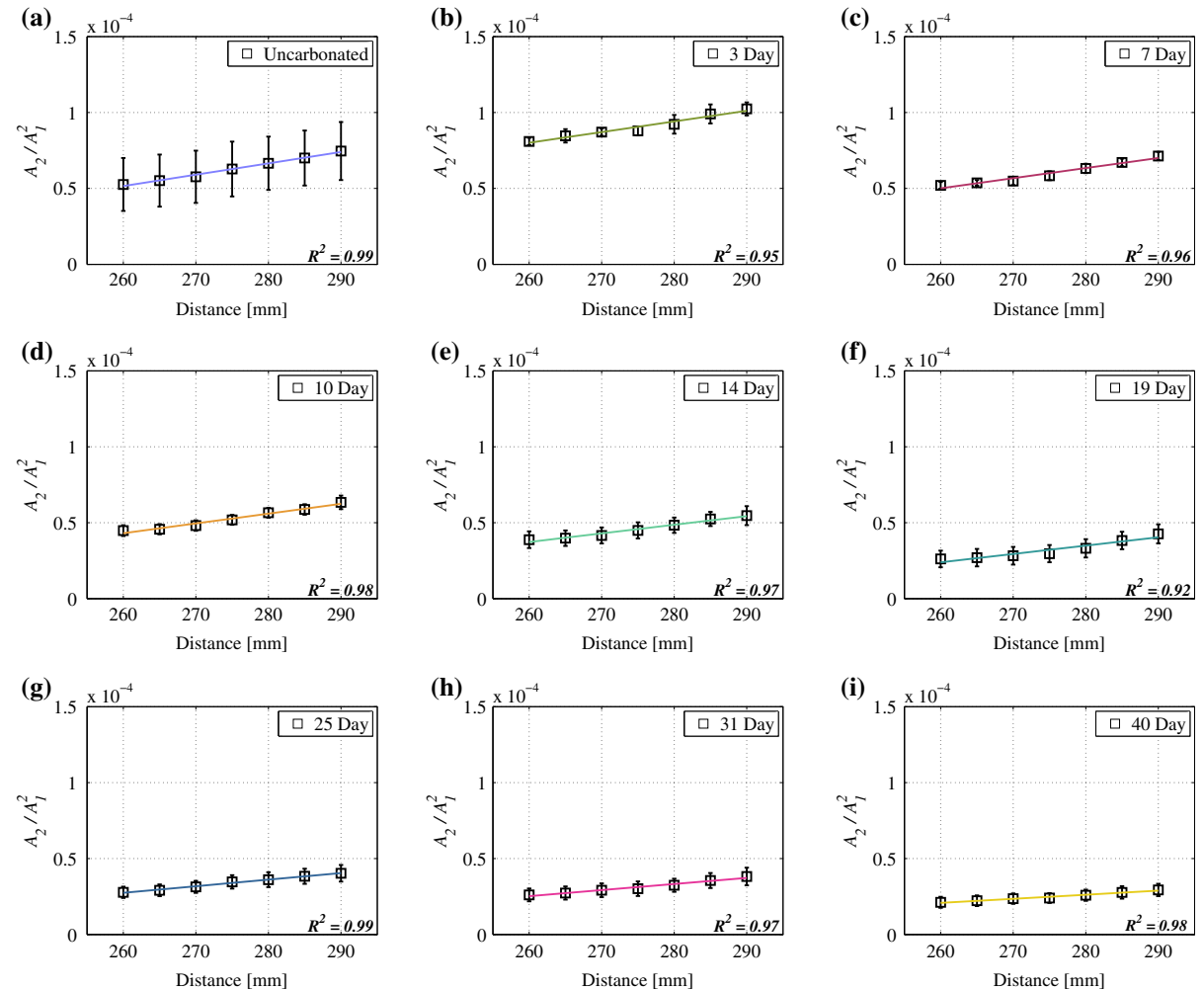
dispersion; a half-space with a finite layer of different material is in general, dispersive. However, our additional measurements on these carbonation specimens demonstrate that the measured velocity difference (velocities at the fundamental versus second harmonic frequencies) is quite small (maximum 4.9 % from the specimen with a 24 mm carbonation layer). Figure 3b also shows a cumulative second harmonic, so the effects of dispersion are negligible and the phase velocity matching of this second harmonic is approximated in this weakly dispersive system at these relatively small propagation distances (0.03 m).

4.3 Acoustic nonlinearity parameter results

The measurement of the SHG in nonlinear Rayleigh surface waves is performed on the concrete specimen as it is exposed to the accelerated carbonation process for 40 days. This measurement uses 45 kHz for the fundamental frequency of the transmitted Rayleigh surface waves. The wavelength at the second harmonic frequency is approximately 27.2 mm, which is greater than the maximum size of the aggregate (MSA) of 12.7 mm so that the measured second harmonic amplitudes are minimally influenced by acoustic scattering. The relative nonlinearity parameter, β_{re} is measured at days 0, 3, 7, 10, 14, 19, 25, 31, and 40. Each data point in Fig. 7 represents an average of the results from 15 to 20 repeated measurements on this specimen. The repeatability of air-coupled detection of the SHG is examined in [38], and the

Table 2 The averaged Rayleigh phase velocity

Exposure time (day)	0	3	7	10	14	19	25	31	40
Phase velocity (m/s)	2,481.84	2,487.17	2,492.71	2,495.57	2,518.57	2,531.37	2,546.04	2,588.22	2,618.94

**Fig. 7** The changes in the slope of the linear fit by the carbonation process

magnitude of the error bars in this figure is mainly due to variations in the contact condition between the wedge transducer (transmitter) and the specimen surface when the wedge transducer is removed and reattached to the specimen for repeated measurements.

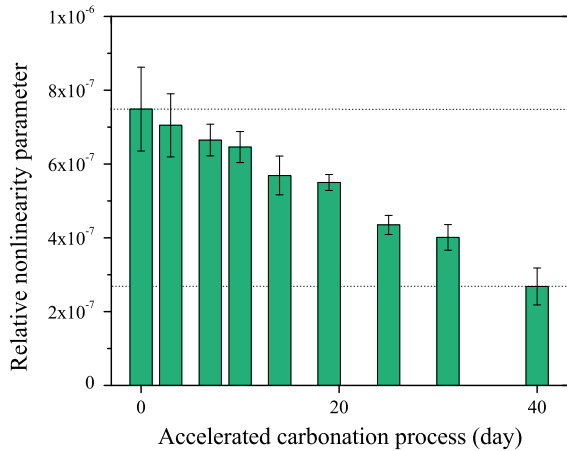
Figure 7 shows the slope of the linear fit of the A_2/A_1^2 versus the propagation distance, which represents β_{re} . Note that all of these β_{re} have R^2 correlation coefficients higher than 0.92. All measured relative nonlinearity parameters, β_{re} during the carbonation

process are listed in Table 3; the measured β_{re} are shown to decrease by a maximum of 64.2 % from that of the uncarbonated concrete specimen. Comparing the results in Figs. 5 and 8, the measured nonlinearity parameters are shown to decrease in a monotonic fashion while the carbonation depth is increasing in an inversely proportional fashion to the nonlinearity parameter. It is interesting to note that the values of β_{re} tend to asymptotically approach a constant value after this maximum measurement period of 40 days



Table 3 The measured relative nonlinearity parameters

Exposure time (day)	0	3	7	10	14	19	25	31	40
Relative nonlinearity parameter ($\times 10^{-7}$)	7.49	7.05	6.65	6.46	5.69	5.50	4.35	4.01	2.68

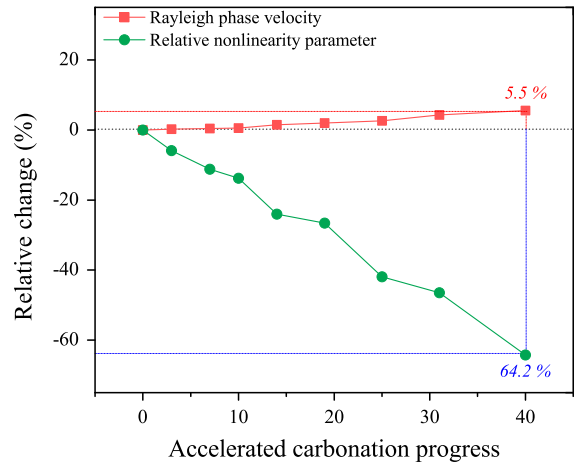
**Fig. 8** Trend of the measured relative nonlinearity parameters and the effect of carbonation on material nonlinearity

since the carbonation depth is almost developed up to the wavelength (~ 27 mm) of the second harmonic Rayleigh surface waves, i.e. beyond this penetration depth, the Rayleigh waves at this frequency lose their sensitivity to the progression of carbonation.

Finally, Fig. 9 compares the relative changes in both the linear and nonlinear parameters, and shows that the sensitivity of the nonlinearity parameter is approximately 12 times higher than that of the Rayleigh phase velocity. More importantly, the relative nonlinearity parameter exhibits a sensitivity high enough to characterize the changes in microstructure, especially the decrease in porosity including filling of microcracks, induced by carbonation. Overall, this research verifies that the SHG technique using nonlinear Rayleigh surface waves provides a promising indicator capable of quantitatively evaluating carbonation in cement-based materials.

4.4 Interpretation of nonlinear ultrasonic measurements

The SHG results highlight that the measured relative nonlinearity parameter is significantly reduced by carbonation and show the sensitivity of the measured nonlinearity parameter to the microstructural changes

**Fig. 9** Sensitivity of nonlinear versus linear ultrasonic parameters

in the carbonated layer. Note that the environmental humidity, CO_2 concentration, and temperature along with the concrete w/c are optimized in this specimen to enhance the carbonation reaction. Based on the nonlinear ultrasonic measurements, it is shown that the carbonation of concrete leads to a reduction in nonlinearity. Most importantly, it is likely that the decrease in the measured relative nonlinearity parameter is mainly attributed to the fact that some pre-existing voids and perhaps some smaller microcracks become filled by CaCO_3 , as described in [54, 55].

5 Conclusion

This paper applies the SHG technique in nonlinear Rayleigh surface waves to concrete to characterize the carbonation-induced microscale behavior of the concrete after exposure to a CO_2 -rich environment, designed to rapidly develop a carbonation front in the concrete. In parallel with the nonlinear ultrasonic measurements which showed a decrease in nonlinearity with carbonation, the destructive characterization using a phenolphthalein indicator solution is performed to track the carbonation depth. The following

conclusions are drawn from these experimental results:

- NDE of the microstructural behavior in the carbonated concrete is achieved by the proposed SHG technique. The relative nonlinearity parameter, β_{re} decreases by as much as 64.2 % after 40 days of curing in the carbonation chamber, and this decrease is attributed to the formation of carbonation product, CaCO_3 which fills pre-existing microcracks, reducing the relative nonlinearity parameter, β_{re} .
- An inverse relationship between the measured carbonation depths and relative nonlinearity parameters is observed.
- It is clearly demonstrated that the relative nonlinearity parameter, β_{re} shows a much higher sensitivity to the carbonation-induced microstructure changes than the measured Rayleigh phase velocity (64.2 vs. 5.5 %). It is therefore expected that the acoustic nonlinearity parameter can be used as a quantitative index for understanding the effect of carbonation if a model that can relate β_{re} to the microstructural changes is available.

Some challenges in the use of NDE to evaluate carbonation still remain to be addressed. These measurements used a relatively low frequency pair (i.e. 50–100 kHz) to reduce the effect of acoustic scattering due to the aggregate. However, more precise characterization could be possible using a range of higher and lower frequency pairs for carbonation penetration.

Acknowledgments The authors gratefully acknowledge the research support from the Electric Power Research Institute (EPRI), Research Project No. 073289.

References

1. Papadakis VG, Vayenas CG (1991) Experimental investigation and mathematical modeling of the concrete carbonation problem. *Chem Eng Sci* 46:1333–1338
2. Papadakis VG, Vayenas CG, Fardis MN (1991) Fundamental modeling and experimental investigation of concrete carbonation. *ACI Mater J* 88:363–373
3. Parrott LJ, Killoh DC (1989) Carbonation in a 36 year old, in situ concrete. *Cem Concr Res* 19:649–656
4. Dow C, Glasser FP (2003) Calcium carbonate efflorescence on Portland cement and building materials. *Cem Concr Res* 33:147–154
5. Bertos MF, Simons SJR, Hills CD, Carey PJ (2004) A review of accelerated carbonation technology in the treatment of cement-based materials and sequestration of CO_2 . *J Hazard Mater B* 112:193–205
6. Monteiro PJM, Clodic L, Battocchio F, Kanitpanyacharoen W, Chae SR, Ha J, Wenk H-K (2013) Incorporating carbon sequestration materials in civil infrastructure: a micro and nano-structural analysis. *Cem Concr Compos* 40:14–20
7. Basheer L, Kropp J, Cleland DJ (2001) Assessment of the durability of concrete from its permeation properties: a review. *Constr Build Mater* 15:93–103
8. Rozière E, Loukili A, Cussigh F (2009) A performance based approach for durability of concrete exposed to carbonation. *Constr Build Mater* 23:190–199
9. Koch GH, Brongers MPH, Thompson NG, Virmani YP, Payer, JH (2002) Corrosion cost and preventive strategies in the United States. Publication no. FHWA-RD-01-156. FHWA, Washington, DC
10. Holland RB (2012) Durability of precast prestressed concrete piles in marine environments. Dissertation, Georgia Institute of Technology
11. Kobayashi K, Suzuki K, Uno Y (1994) Carbonation of concrete structures and decomposition of C-S-H. *Cem Concr Res* 24:55–61
12. Villain G, Platret G (2006) Two experimental methods to determine carbonation profiles in concrete. *ACI Mater J* 103:265–271
13. Thiery M, Villain G, Dangla P, Platret G (2007) Investigation of the carbonation front shape on cementitious materials: effects of the chemical kinetics. *Cem Concr Res* 37:1047–1058
14. Moorehead DR (1986) Cementation by the carbonation of hydrated lime. *Cem Concr Res* 16:700–708
15. Vanzo J (2009) A nanochemomechanical investigation of carbonated cement paste. Master thesis, Massachusetts Institute of Technology
16. Johannesson B, Utgenannt P (2001) Microstructural changes caused by carbonation of cement mortar. *Cem Concr Res* 31:925–931
17. Jerga J (2004) Physico-mechanical properties of carbonated concrete. *Constr Build Mater* 18:645–652
18. Khan MI, Lynsdale CJ (2002) Strength, permeability, and carbonation of high-performance concrete. *Cem Concr Res* 32:123–131
19. Atiş CD (2003) Accelerated carbonation and testing of concrete made with fly ash. *Constr Build Mater* 17:147–152
20. Torgal FP, Miraldo S, Labrincha JA, Brito JD (2012) An overview on concrete carbonation in the context of eco-efficient construction: evaluation, use of SCMs and/or RAC. *Constr Build Mater* 36:141–150
21. Younsi A, Turcry P, Rozière E, Ait-Mokhtar A, Loukili A (2011) Performance-based design and carbonation of concrete with high fly ash content. *Cem Concr Compos* 33:993–1000
22. Papadakis VG (2000) Effect of supplementary cementing materials on concrete resistance against carbonation and chloride ingress. *Cem Concr Res* 30:291–299
23. Kamali S, Moranville M, Leclercq S (2008) Material and environmental parameter effects on the leaching of cement pastes: experiments and modelling. *Cem Concr Res* 38:575–585



24. Kobayashi K, Uno Y (1990) Influence of alkali on carbonation of concrete, part 2-influence of alkali in cement on rate of carbonation of concrete. *Cem Concr Res* 20:619–622
25. Papadakis VG, Fardis MN, Vayenas CG (1992) Effect of composition, environmental factors and cement-lime mortar coating on concrete carbonation. *Mater Struct* 25:293–304
26. De Schutter G, Audenaert K (2004) Evaluation of water absorption of concrete as a measure for resistance against carbonation and chloride migration. *Mater Struct* 37:591–596
27. Fattuhi NI (1988) Concrete carbonation as influenced by curing regime. *Cem Concr Res* 18:426–430
28. Rostami V, Shao Y, Boyd AJ, He Z (2012) Microstructure of cement paste subject to early carbonation curing. *Cem Concr Res* 42:186–193
29. Kobayashi K, Uno Y (1989) Influence of alkali on carbonation of concrete, part 1, preliminary tests with mortar specimen. *Cem Concr Res* 19:821–826
30. Popovics JS, Song WJ, Ghandehari M, Subramaniam KV, Achenbach JD, Shah SP (2000) Application of surface wave transmission measurements for crack depth determination in concrete. *ACI Mater J* 97:127–135
31. Popovics S, Rose JL, Popovics JS (1990) The behavior of ultrasonic pulses in concrete. *Cem Concr Res* 20:259–270
32. In C-W, Holland RB, Kim J-Y, Kurtis KE, Kahn LF, Jacobs LJ (2013) Monitoring and evaluation of self-healing in concrete using diffuse ultrasound. *NDT&E Int* 57:36–44
33. Selleck SF, Landis EN, Peterson ML, Shah SP, Achenbach JD (1998) Ultrasonic investigation of concrete with distributed damage. *ACI Mater J* 95:27–36
34. Chen J, Jayapalan AR, Kim J-Y, Kurtis KE, Jacobs LJ (2010) Rapid evolution of alkali-silica reactivity of aggregates using a nonlinear resonance spectroscopy technique. *Cem Concr Res* 40:914–923
35. Leśnicki KJ, Kim J-Y, Kurtis KE, Jacobs LJ (2011) Characterization of ASR damage in concrete using nonlinear impact resonance acoustic spectroscopy technique. *NDT&E Int* 44:721–727
36. Leśnicki KJ, Kim J-Y, Kurtis KE, Jacobs LJ (2013) Assessment of alkali-silica reaction damage through quantification of concrete nonlinearity. *Mater Struct* 46:497–509
37. Bouchaala F, Payan C, Garnier V, Balayssac JP (2011) Carbonation assessment in concrete by nonlinear ultrasound. *Cem Concr Res* 41:557–559
38. Kim G, In C-W, Kim J-Y, Kurtis KE, Jacobs LJ (2014) Air-coupled detection of nonlinear Rayleigh surface waves in concrete-application to microstructure characterization. *NDT&E Int* 67:64–70
39. Herrmann J, Kim J-Y, Jacobs LJ, Qu J, Littles JW, Savage MF (2006) Assessment of material damage in a nickel-base super alloy using nonlinear Rayleigh surface waves. *J Appl Phys* 99:124913
40. Walker SV, Kim J-Y, Qu J, Jacobs LJ (2012) Fatigue damage evaluation in A36 steel using nonlinear Rayleigh waves. *NDT&E Int* 48:10–15
41. Ruiz A, Ortiz N, Medina A, Kim J-Y, Jacobs LJ (2013) Application of ultrasonic methods for early detection of thermal damage in 2205 duplex stainless steel. *NDT&E Int* 54:19–26
42. Thiele S, Kim J-Y, Qu J, Jacobs LJ (2014) Air-coupled detection of nonlinear Rayleigh surface waves to assess material nonlinearity. *Ultrasonics* 54:1470–1475
43. Kim G, In C-W, Kim J-Y, Jacobs LJ, Kurtis KE (2014) Nondestructive detection and characterization of carbonation in concrete. *Rev Prog Quant Nondestr Eval* 1581:805–813
44. Zeitvogel DT, Matlack KH, Kim J-Y, Jacobs LJ, Singh PM, Qu J (2014) Characterization of stress corrosion cracking in carbon steel using nonlinear Rayleigh surface waves. *NDT&E Int* 62:144–152
45. Mehta PK, Monteiro PJM (2006) *Concrete: microstructure, properties, and materials*, 3rd edn. McGraw-Hill, New York
46. Viktorov IA (1967) *Rayleigh and Lamb waves*. Plenum Press, New York
47. Matlack KH, Kim J-Y, Jacobs LJ, Qu J (2015) Review of second harmonic generation measurement techniques for material state determination. *J Nondestruct Eval*. doi:10.1007/s10921-014-0273-5
48. Huang CL (2013) Effect of beam diffraction on nonlinear Rayleigh surface wave measurements. Master thesis, Georgia Institute of Technology
49. Torello D, Thiele S, Matlack KH, Kim J-Y, Qu J, Jacobs LJ (2015) Diffraction, attenuation, and source corrections for nonlinear Rayleigh wave ultrasonic measurements. *Ultrasonics* 56:417–426
50. ACI Committee 211 (1991) Standard practice for selecting proportions for normal, heavyweight, and mass concrete (AU 211.1-91). ACI, Detroit, p 38
51. ASTM C 150-04 (2004) Standard specification for Portland cement. ASTM, PA
52. Bertolini L, Elsener B, Pedferri P, Polder RB (2004) *Corrosion of steel in concrete: prevention diagnosis, repair*. Wiley-VCH, Weinheim
53. Kim J-Y, Jacobs LJ, Qu J, Littles JW (2006) Experimental characterization of fatigue damage in a nickel-base super-alloy using nonlinear ultrasonic waves. *J Acoust Soc Am* 120:1266–1273
54. Hearn N (1998) Self-sealing, autogenous healing and continued hydration: what is the difference? *Mater Struct* 31:563–567
55. Edvardsen C (1999) Water permeability and autogenous healing of cracks in concrete. *ACI Mater J* 96:448–454